Journal of Cleaner Production 418 (2023) 138127

Contents lists available at ScienceDirect

Journal of Cleaner Production

journal homepage: www.elsevier.com/locate/jclepro

Process assessment of renewable-based acrylic acid production from glycerol valorisation

Aya Sandid [a], Jesús Esteban [a], Carmine D'Agostino [a,b], Vincenzo Spallina [a,*]

[a] Department of Chemical Engineering, School of Engineering, University of Manchester, Manchester, M13 9PL, United Kingdom
[b] Dipartimento di Ingegneria Civile, Chimica, Ambientale e dei Materiali (DICAM), Università di Bologna, 40131 Bologna, Italy

ARTICLE INFO

Handling Editor: Panos Seferlis

Keywords:
Glycerol
Acrylic acid
Acrolein
Techno-economic analysis
Process simulation

ABSTRACT

The continuous growth of biodiesel production *via* transesterification is leading to an increase in the generation and availability of the by-product glycerol. In this study, a glycerol-based process for the production of acrylic acid has been designed and simulated. The valorisation of glycerol route includes a two-step conversion process where glycerol is first dehydrated to acrolein and acrolein is selectively oxidised to acrylic acid. This renewable-based process is then compared in terms of heat integration and techno-economic performance to the traditional petrochemical route from propylene from a techno-economic and environmental point of view. The study includes the detailed design of the separation train in which azeotropic distillation is also assessed along with the sensitivity analysis of the most relevant variables of the process. Using a production basis of approximately 10,250 kg h^{-1} of acrylic acid (purity>99.5 wt%), results show that the glycerol route generates 37.3% less CO_2 emissions than the propylene-based. From the heat integration analysis, slightly lower heating (96.6%) but higher cooling (32.4%) energy savings can be attained in the glycerol route as opposed to heating (100%) and cooling (21.6%) energy savings available in the propylene-based route. In terms of economics, the glycerol-based route has a lower capital expenditure (£74.0 million) and operating expenditure (£171.4 million yr^{-1}) compared to the propylene route (£91.3 million and £180.2 million yr^{-1}, respectively). Nevertheless, considering the use of raw material and its cost, the glycerol route is more demanding (1.96 kg h^{-1} of pure glycerol per kg h^{-1} of acrylic acid amounting to £138.6 million yr^{-1}) than the propylene route (0.92 kg h^{-1} of propylene per kg h^{-1} of acrylic acid at £117.2 million yr^{-1}).

1. Introduction

As the global economy continues to grow, the world's energy consumption is also increasing (U.S. Energy Information Administration (EIA), 2021), and it is expected to increase by 50%–900 quadrillion Btu in 2050 (U.S. Energy Information Administration (EIA), 2019). Hence, the search for new sustainable sources that can satisfy the energy demand whilst also ensuring environmental conservation is becoming imperative (Cornejo et al., 2017). Thus, increasing attention towards the generation of potential energy sources such as hydrogen (Stenberg et al., 2021) and biofuels, among which biodiesel has been implemented as an alternative to fossil fuels (Attarbachi et al., 2023).

Biodiesel is a liquid fuel, currently produced *via* the transesterification of triglycerides with alcohols, mostly methanol, to generate fatty acid alkyl esters (biodiesel) together with crude glycerol as a by-product. For every tonne of biodiesel, approximately 100 kg of glycerol is also produced from the reaction (Wu et al., 2020) as a by-product. various studies investigated different routes to valorise glycerol such as selective oxidation, carboxylation, acetalization, and dehydration to generate high-value chemicals such as glyceric acid (Choi et al., 2022), glycerol carbonate (Esteban et al., 2015), solketal (Esteban et al., 2015), and acrolein (Liu et al., 2012), respectively. Glycerol composition varies (30–60% in weight) according to the feedstock used for the transesterification reaction with 10–19% of ash, ≤10% of water, and ≤40% of matter organic non-glycerol (MONG) (Attarbachi et al., 2023). It was found that especially alkali metal ions cause catalyst deactivation and therefore it affects product yield, MONG content however, had a minor effect on yield (Dimian et al., 2019), and a similar behaviour in the case of etherification of glycerol with benzyl alcohol, using treated crude glycerol (i.e purified glycerol) as a feedstock (Pico et al., 2013). This was also observed when studying the production of lipids as it was concluded that purified glycerol as a medium led to similar results (i.e lipid yield) as if pure glycerol was used as the raw

* Corresponding author.
E-mail address: vincenzo.spallina@manchester.ac.uk (V. Spallina).

https://doi.org/10.1016/j.jclepro.2023.138127
Received 6 March 2023; Received in revised form 11 June 2023; Accepted 15 July 2023
Available online 16 July 2023

Nomenclature and abbreviations

AA	Acrylic Acid
CAGR	Compound Annual Growth Rate (%)
CAPEX	Capital Expenditure (£)
CEPCI	Chemical Engineering Plant Cost Index
DIPE	Diisopropyl Ether
GCC	Grand Composite Curve
HEN	Heat Exchanger Network
LHV	Lower Heating Value (MJ kg^{-1})
LL	Liquid-Liquid
MONG	Matter Organic Non-Glycerol
NRTL	Non-Random Two-Liquid model
NRTL-HOC	Non-Random Two-Liquid model (Hayden-O'Connell)
OPEX	Operating Expenditure (£ yr^{-1})
P&ID	Piping & Instrumentation diagram
PFR	Plug Flow Reactor
RSTOIC	Stoichiometric Reactor
UNIQUAC	Universal Quasi-Chemical model

material (R Kumar et al., 2020; Kumar et al., 2021). The conversion of glycerol to acrolein specifically has gained attention due to it being a vital intermediate to many high-value chemicals such as glutaraldehyde, allyl alcohol, 1,3-propanediol, and acrylic acid (AA) (Arntz et al., 2007). AA is a valuable component as it is converted to generate high-value polymers and acrylate esters, which are then further utilised to manufacture hygiene and personal care products, adhesives, textiles, coatings, paints, plastics, wastewater treatment chemicals, detergents, flocculants, and thickeners (Brown, 2014). Due to high demand, the global market of AA is expected to grow at a CAGR of 4.8% from $12.0 billion in 2020 to $19.92 billion in 2030 (Bhagyashri Patil, 2022) (Ruy, 2020) (IHS Markit, 2020). Currently, AA is manufactured *via* the two-step catalytic oxidation of propylene (Ohara et al., 2020). In this route, propylene first undergoes a gas phase reaction (1) in which it is oxidised to the intermediate product acrolein in the presence of air and steam (Ohara et al., 2020) at a demanding temperature between 300 °C and 400 °C (Arntz et al., 2007). Acrolein is then further oxidised in a gas phase reaction (2) to generate AA (Ohara et al., 2020). at operating conditions of 200–300 °C (Ohara et al., 2020).

$$C_3H_6 + O_2 \rightarrow C_3H_4O + H_2O \quad \Delta H^0 = -340.8\ kJ\ mol^{-1}_{C_3H_6} \tag{1}$$

$$C_3H_4O + \frac{1}{2}O_2 \rightarrow C_3H_4O_2 \quad \Delta H^0 = -254.1\ kJ\ mol^{-1}_{C_3H_4O}\# \tag{2}$$

There is potential in generating AA in a single-step process (3), in which propylene is converted directly to AA (Dimian et al., 2019), nevertheless, this process is currently unsuitable for implementation as the catalyst utilised usually has a short lifetime and the process tends to generate AA with a yield of 50–60% (Ohara et al., 2020).

$$C_3H_6 + \frac{3}{2}O_2 \rightarrow C_3H_4O_2 + H_2O \quad \Delta H^0 = -594.9\ kJ\ mol^{-1}_{C_3H_6} \tag{3}$$

Alternatively, the glycerol-based route is also a two-step process, in which glycerol undergoes a dehydration reaction (4) to generate acrolein in the presence of a silicotungstic acid catalyst and operating conditions of 300–350 °C (Dimian et al., 2019). Acrolein is then further oxidised (reaction (2)) in a different reactor to generate AA as in the propylene-based route.

$$C_3H_8O_3 \rightarrow C_3H_4O + 2H_2O \quad \Delta H^0 = 12.46\ kJ\ mol^{-1}_{C_3H_8O_3} \tag{4}$$

Dimian and Bildea (2021) investigated four fluidised bed reactor configurations in which the dehydration reaction occurs which have resulted in lower gas emissions compared to the current propylene processes. Song et al. (2020) proposed a design in which a fermentation reactor followed by a catalytic reactor is used to generate AA where liquid-liquid extraction using toluene resulted in the most efficient solution. Braga et al. (2020) proposed an economically feasible design in which the single-step oxidation dehydration reaction generates acrylic acid although there is little evidence that this process is feasible. Finally, Sánchez-Gómez et al. (2022) proposed a process in which AA is generated via reactive distillation leading to a 74% reduction in heat duty consumption compared to AA conventional processes.

Although current literature proposes some designs for the production of AA from glycerol, there is a gap in the industrial economics analysis, using the same metrics for the comparison of the two routes and the impact of more efficient and high performing reactors and separation process is not fully understood despite the efforts devoted in developing new materials and more intensified reactors. In this paper, the comprehensive appraisal of the techno-economic performance, heat integration and CO_2 (direct and indirect) emissions are assessed for both processes. Moreover, the economic analysis is taking into consideration the different costs and financial aspects generated post-COVID and thus provides a more reliable cost analysis.

2. Methods

2.1. Thermodynamic model and Assumptions

Process simulations are performed using Aspen Plus V11.0. The plants were simulated assuming continuous operation for 8000 h per year (Suo et al., 2015) and generate about 82,000 tons annually of AA (10,250 kg h^{-1}) with 99.5% wt. purity (Ohara et al., 2020).

The thermodynamic package set for all units within the propylene-based process is UNIQUAC (Alvarez et al., 2007) and NRTL-HOC for the glycerol-based process (Dimian et al., 2019). NRTL was set for the final separation unit in both processes, where AA present in a diluted solution is separated from water (Song et al., 2020). It was assumed that all heat exchangers are shell and tube and have a pressure drop of 2% (of the inlet pressure) and all compressors isentropic efficiency of 75%. Low-pressure steam is assumed to be 160 °C and 6.0 bar (Luyben, 2016).

Regarding the raw material streams, chemical grade propylene (94 mol%, C_3H_6, 3% C_2H_6 and 3% C_3H_8) at 25 °C and 11.5 bar (Petrescu et al., 2016) (Premlall and Lokhat, 2020). Crude glycerol cannot be used directly for catalytic conversion to high-value chemicals (Xiao et al., 2013), therefore, this study assumed that purified glycerol is comparable to pure glycerol which is utilised as a raw material. The inlet stream was set as a solution containing 85 wt% pure glycerol and 15 wt% of water (Dimian et al., 2019). The integration of the upstream process for glycerol purification from bio-diesel plants can vary substantially and therefore this part has been considered out of the scope of the current investigation which is looking at the conversion of glycerol into acrylic acid.

The kinetic models applied in this study are based on previous experimental studies and more specifically propylene to acrolein (Redlingshöfer et al., 2003), glycerol to acrolein (Talebian-Kiakalaieh A., 2017), and acrolein to AA (Drochner et al., 2014). The conversion of glycerol to AA is carried out following the design suggested by (Dimian et al., 2019) for the base case.

2.2. Kinetic models

All kinetic values were validated against the experimental data available in literature. For the conversion of propylene to acrolein over a bismuth molybdate catalyst, the reactions and kinetics detailed in Table S1 in section A of the supplementary information and the model are validated with a previous study by (Redlingshöfer et al., 2003). Kinetics were validated using a PFR at isothermal conditions at a temperature of 370 °C which replicate the experimental system in the reference. Because the process is carried out at temperature above

360 °C power-law kinetics was considered the rate-determining step (Redlingshöfer et al., 2002, 2003). For the conversion of acrolein to AA, over a molybdenum/vanadium mixed oxide (Table S2 in section A in the supplementary information) the model validated against the experiments in Drochner et al., (2014) was validated. In the case of the conversion of glycerol to acrolein over a silicotungstic acid catalyst (Table S3 in section A in the supplementary information), the kinetic model is based on the study by Talebian-Kiakalaieh (2017).

3. - Process description

3.1. Propylene-based process

The process flow diagram of the process is shown in Fig. 1. The process starts by mixing propylene (1), air (3) and steam (2) at molar ratio of 1:10.7:4 (Luyben, 2016). The air stream is compressed from 1.01 bar to 3.67 bar. The mixed raw materials (6) are heated to 366 °C (7) before entering the 1st reactor (PR_1) where propylene is oxidised to acrolein, and then acrolein is oxidised to AA. The cooled stream (11) enters the quenching unit (P_A1) with fresh water (12) to eliminate non-condensable gases and generate an AA aqueous solution (Ohara et al., 2020).

The aqueous solution (14) then enters a liquid-liquid extractor (P_E1), in which diisopropyl ether (DIPE) is utilised as a solvent due to its insolubility in water and its effectiveness in extracting AA from water (Alvarez et al., 2007). The extract stream (17) enters a solvent recovery column (P_D1) that operates at 0.3 bar (Dimian et al., 2019) to generate a vapor distillate rich in DIPE. The distillate is further processed in a flash vessel operating at 5 °C to separate any remaining non-condensable gases. The liquid product from the flash vessel enters a decanter operating at 75 °C (and vacuum) to separate water and DIPE. The water product is returned to the column (P_D1) as external reflux and the lean DIPE (23) is recycled back to the extractor. Finally, the bottoms product from the distillation column (25), is free of solvent, mainly consisting of AA, acetic acid, and water, which enters another distillation column (P_D3) for further purification. The raffinate stream (18) is also further processed in a raffinate stripper (P_D2) to recover and recycle any remaining solvent back to the extractor.

The solvent recycle stream combines the DIPE streams generated from the solvent recovery column (24) and the raffinate stripper (28). The flow rate of DIPE was set based on the ratio of DIPE to AA of 3.6 (Dimian et al., 2019).

Finally, a vacuum distillation column (P_D3 operated at 0.10 bar) is used to further purifies the AA stream from previous purification step (25) at the required purity.

In addition, fired heaters were simulated to process the waste gases/purge streams generated from the absorber (P_A1) and the flashes. The air flowrate (streams 15, 26 and 34) used for combustion was set so that about 6 mol% of excess oxygen is left in the flue gas to ensure proper combustion (A.Vallero, 2019).

3.2. Glycerol-based process

The process flow diagram of the process is shown in Fig. 2. Glycerol (1), air (5), and H_2O (3) are pre-heated separately and they are fed to the dehydration reactor (G_R1), where glycerol is converted to acrolein according to the suggested feed conditions reported in the literature (Dimian et al., 2019).

The product stream generated enters the distillation column (G_D1) to eliminate heavy components such as acetol and propionic acid produced whilst recovering acrolein completely in the distillate before entering the oxidation reactor. This is due to the close boiling points of AA (141.0 °C), acetol (145.4 °C), and propionic acid (141.2 °C) at atmospheric pressure.

The distillate (9) mainly consisting of acrolein is mixed with additional air (11) and then enters the oxidation reactor (G_R2) where AA is produced. The AA product is cooled to 40 °C *via* the heat exchanger to stop the occurrence of further side reactions. The two-phase stream is separated at 5.0 bar and the vapours (16) are quenched in an absorption column (G_A1) with fresh water (18) to remove the non-condensable gases and generate an AA solution (21), which is then mixed with the liquid phase stream (17) generated from the flash.

The resulting solution enters the product recovery unit (G_D2). Due to the formation of water azeotropes (water-AA and water-acetic acid). Azeotropic distillation has been employed and simulated for the glycerol-based route as a more advanced alternative to LL extraction. This is done to compare the effectiveness of implementing advanced separation (azeotropic distillation) to conventional separation methods

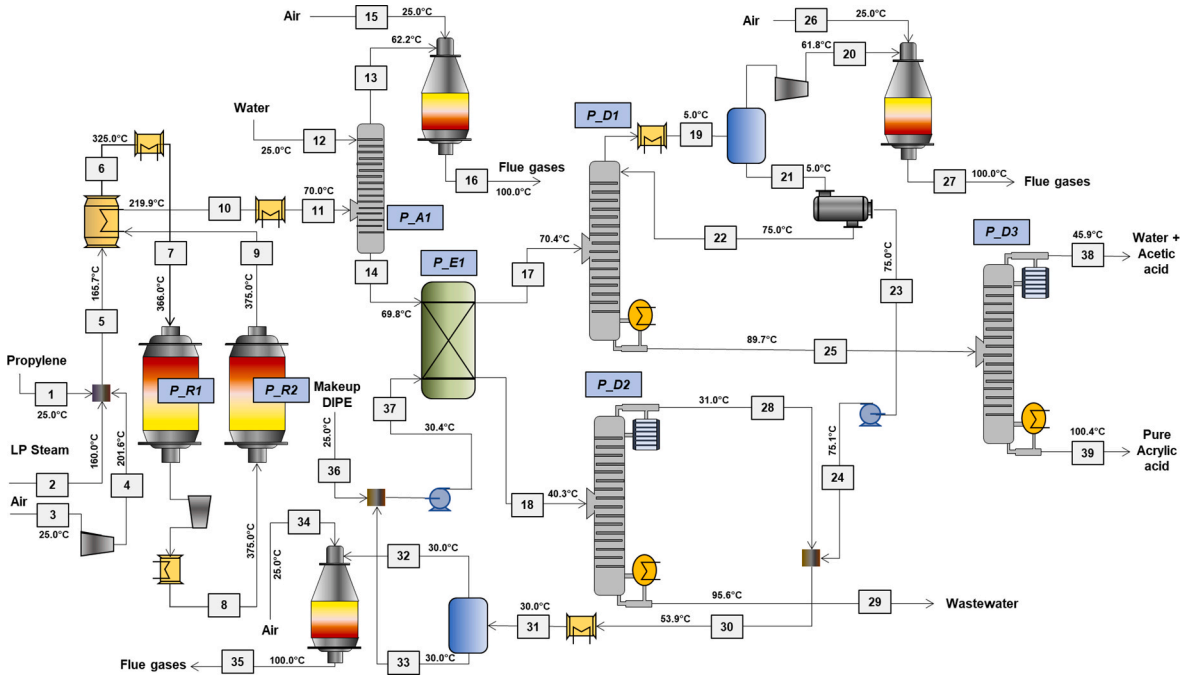

Fig. 1. Flow diagram for the propylene-based process.

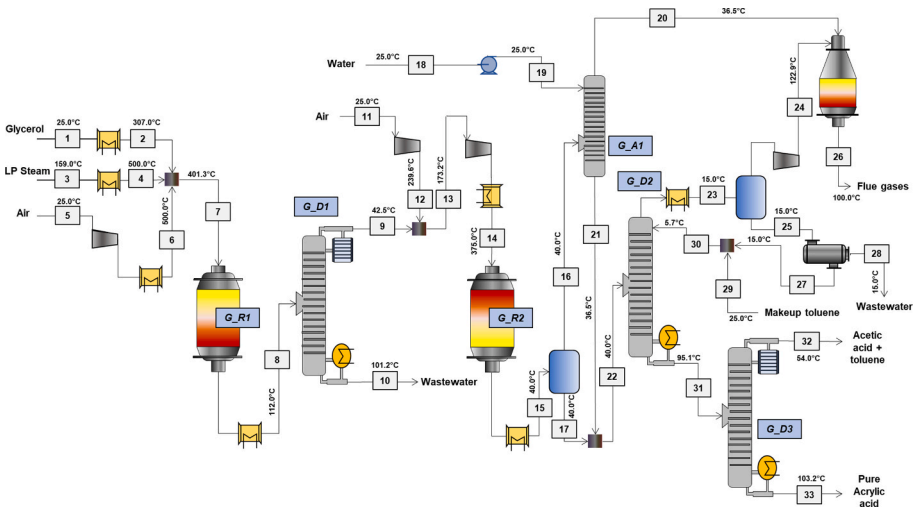

Fig. 2. Flow diagram for the glycerol-based process.

(LL extraction). Toluene is utilised as an entrainer due to its immiscibility in water. The column (G_D2) generates a vapor distillate which mainly consists of toluene and water, which is recycled back into the column after flashing the stream at sub-atmospheric pressure 0.3 bar. The bottoms product (31) which consists of AA enters the final distillation column (G_D3), which is operating at a high vacuum (0.1 bar), for purification. A fired heater is used to process the waste gases/purge streams generated from the absorber (G_A1) and the flash.

3.3. Heat integration (pinch analysis)

To investigate energy saving opportunities, pinch analysis (Smith, 2005) was performed *via* the software SPRINT (University of Manchester, 2022). The heating and cooling streams from the separation units, heat exchangers and PFR reactors (described in Table 6) are considered in the optimisation to obtain the minimum energy requirement of the process by assuming a minimum temperature approach of 10 °C. The details of the heat integration data are reported in Section E of the supplementary information.

In the case of cooling duty with the need for refrigeration, a minimum ΔT of 5 °C is considered with a Carnot efficiency of 60% according to the methodology reported in (Smith, 2005).

3.4. Economic analysis

Economic Analysis was performed for both processes. The analysis includes the calculation of the capital expenditure (CAPEX), operating expenditure (OPEX), and profits.

CAPEX was calculated *via* the factorial method (Sinnott and Towler, 2020). Details of the equipment sizing data are illustrated in Tables S14 and S15 in section F in the supplementary information. Costs are actualised to May 2022 using the Chemical Engineering Plant Cost Index (CEPCI) 831.1 (May 2022 as reported in (Chemical Engineering, 2022). Working capital and start-up costs were calculated assuming they represent 10% each of the total capital cost (Sinnott and Towler, 2020). These added up to the total investment cost (TIC).

The cost of the raw materials and utilities in the UK are shown in Table 1; it should be noted that due to the lack of AA price availability in the UK, the average AA price across the world was calculated and taken using the data for March 2022. Other relevant data are available in Table 2 including also the CO_2 emission tax is implemented at £50 $ton^{-1}_{(CO_2)}$ (Department for Business Energy and Industrial Strategy, UK, 2020).

A sensitivity analysis was performed to investigate the effect of varying the cost of propylene, glycerol, and AA on the total profits. This was achieved by decreasing and increasing the cost of the components from 0% to 30% and observing the effect on the profits.

Table 1
Cost of raw materials and utilities.

Component	Cost	Reference
Raw Materials		
Propylene (£ ton^{-1})	1123.4	ChemAnalyst (2022c)
Pure glycerol (£ ton^{-1})	645.6	Chilakamarry et al. (2021)
DIPE (£ ton^{-1})	1681.0	ChemAnalyst (2022b)
Toluene (£ ton^{-1})	1087.9	Echemi Technology (2022)
Products		
AA (£ ton^{-1})	2025.4	ChemAnalyst (2022a)
Utilities		
Electricity (£ kWh^{-1})	0.21	(Department for Business, 2022)
Natural Gas (£ MWh^{-1})	43.7	(Department for Business, 2022)
Low-Pressure Steam (£ ton^{-1})	5.7	Brennan (2020)
Distilled water (£ ton^{-1})	0.8	Brennan (2020)
Cooling water (£ ton^{-1})	0.1	Brennan (2020)

Table 2
Labour costs.

	Shifts	Number of people per shift	Total	Salary (£ yr^{-1})	Reference
Plant Operator	3	6	18	27,639	(Indeed, 2022d)
Plant manager	3	2	6	40,028	(Indeed, 2022c)
Maintenance technicians	1	6	6	29,285	(Indeed, 2022b)
Maintenance engineers	1	2	2	35,922	(Indeed, 2022a)

4. - Results

4.1. Kinetic model validation

4.1.1. Propylene-based process

Table 3 and Table 4 present the results of the kinetic validation for the conversion of propylene to acrolein and acrolein to AA, respectively. The validation was carried out by simulating the same reactor geometry and operating conditions as presented in literature. For the conversion of propylene to acrolein, the reactions' orders set, presented in the

Table 3
Kinetic validation results using Aspen Plus for the conversion of propylene to acrolein.

Component	Variable	Simulation results (%)	Reference (Redlingshöfer et al., 2002) results (%)	Error (%)
Propylene	Conversion	56.90	60.3	5.6
Acrolein	Selectivity	92.05	89.5	2.8

Table 4
Kinetic validation results using Aspen Plus for the conversion of acrolein to AA.

Component	Variable	Simulation results (%)	Reference (Drochner et al., 2014) results (%)	Error (%)
Acrolein	Conversion	81.9	81.0	1.1
AA	Selectivity	79.9	76.0	5.1
Carbon Dioxide	Selectivity	11.8	11.8	0.0

supplementary information section A, are in the range of 0–1, which is within the typical range for heterogeneously catalytic reactions (Redlingshöfer et al., 2003) and confirmed also in (Premlall and Lokhat, 2020). For the conversion of acrolein to AA, the partial order of each component was set to 1, resulting in a second order reaction (Drochner et al., 2014). It should be noted that the model (i.e pre-exponential factors) suggested by (Drochner et al., 2014) was fitted to achieve acceptable percentage errors. The modified model is presented in the supplementary information section A since the model presented was reporting several terms which could not be implemented in Aspen (O_2 isotopes terms). The results achieved from the simulations were compared to previous experimental results (Drochner et al., 2014; Redlingshöfer et al., 2002) by calculating the absolute differences and percentage errors.

For the case of the conversion of propylene to acrolein (Table 3) the deviation can be assumed to have a negligible effect on subsequent results as acrolein deviates by 2.8% which has been considered acceptable because some uncertainties are associated on the simulation. For side reactions, given the low selectivity, hence low flowrates and fraction in the product, the errors can be very high however, for the purpose of this work it was considered acceptable in view of the sensitivity analysis carried out later on and very low impact on the process M&H balances.

4.1.2. Glycerol-based process

The kinetic model is illustrated in Table S3 in the supplementary information and differences with the results in (Talebian-Kiakalaieh A., 2017) in Table 5. The same model has been used also by (Dimian et al., 2019) in their study on a large scale.

4.2. Optimisation results (equipment sizing)

Table 6 shows the optimisation results for the reactors in terms of reactor length, diameter and number of tubes for an isothermal system. The ratio of length to diameter (L/D) was set to 5. The objective function was set to achieve the maximum conversion of the main components (propylene, glycerol and acrolein). The diameter and length of the tubes for the reactor P_R1 were constrained to be 0.05 m and 5 m, while for the other reactors, diameter and length were constrained to 5 m and 15 m maximum, respectively which is typical industrial standards as the ease of transporting equipment must be considered during the mechanical design of the reactors.In addition, as the glycerol dehydration reactor (G_R1) operates adiabatically, a sensitivity analysis shown in Fig. 3 was done to illustrate the effect of temperature on acrolein generated from the reactor. It is observed that increasing the inlet temperature from 365 °C to 401 °C, lead to an increase in acrolein production by 172 kg h^{-1}. However, further increasing the inlet temperature to 436 °C, lead to acrolein reduction by 41 kg h^{-1} due to an increase in the generation of the side products (i.e. propionic acid and acetone).

Table 7 and Table 8 show column sizing results in the propylene and

Table 5
Validation of the kinetic model according to the experimental results in (Talebian-Kiakalaieh A., 2017) at different temperatures for a contact time of 1.5 × $10^3 \frac{kg_{cat} \bullet s}{m^3}$.

Component/ variable	Simulation results (%)	(Talebian-Kiakalaieh A., 2017) results (%)	Error (%)
Glycerol conversion (280 °C)	79.2%	82.0%	3.4
Acrolein selectivity (280 °C)	83.8%	79.3%	5.7
Glycerol conversion (300 °C)	89.2%	90.0%	0.9
Acrolein selectivity (300 °C)	83.3%	80.0%	4.1
Glycerol conversion (320 °C)	95.4%	94.0%	1.5
Acrolein selectivity (320 °C)	82.6%	79.8%	3.6
Glycerol conversion (340 °C)	98.5%	98.0%	0.5
Acrolein selectivity (340 °C)	81.9%	78.6%	4.2

Table 6
Reactor sizing in both processes.

	P_R1	P_R2	G_R1	G_R2
Operation Mode	Isothermal	Isothermal	Adiabatic	Isothermal
Temperature (°C)	366	375	401–375	375
Pressure (bar)	3.7	7	4	5
Length (m)	2.90	9.5	5.8	11.0
Diameter (m)	0.049[a)]	1.9	1.16	2.2
Number of Tubes	1750	–	–	–
Bed voidage	0.138	0.67	0.53	0.67

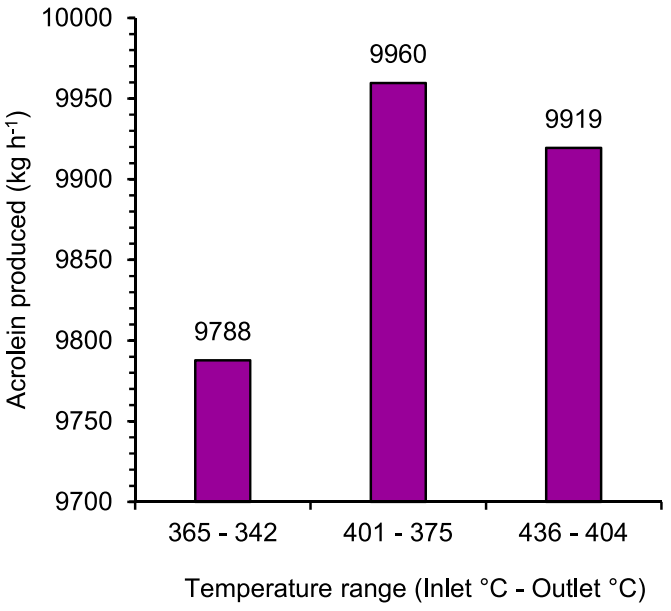

Fig. 3. Effect of reactor's (G_R1) temperature on acrolein production.

Table 7
Column sizing for the propylene-based process.

	P_A1	P_E1	P_D1	P_D2	P_D3
Model	RadFrac	Extract	RadFrac	RadFrac	RadFrac
Condenser	None	–	None	Partial-Vapor	Total
Reboiler	None	–	Kettle	Kettle	Kettle
Number of Stages	10	8	50	8	30
Stage 1 pressure (bar)	6.80	6.86	0.30	1.01	0.1
Final Stage pressure (bar)	6.86	6.91	0.62	1.06	0.245
Distillate rate (kmol h^{-1})	–	–	693.7	30.2	293.6
Reflux ratio	–	–	–	0.047	3.5
Feed Stage	–	–	25	4	15

Table 8
Column sizing for the glycerol-based process.

	G_D1	G_A1	G_D2	G_D3
Model	RadFrac	RadFrac	RadFrac	RadFrac
Condenser	Partial-Vapor	None	None	Total
Reboiler	Kettle	None	Kettle	Kettle
Number of Stages	8	6	12	20
Stage 1 pressure (bar)	1.00	4.97	0.30	0.150
Final Stage pressure (bar)	1.045	5.00	0.37	0.274
Distillate rate (kmol h^{-1})	309.0	–	240.0	31.3
Reflux ratio	3	–	–	4
Feed Stage	4	–	6	10

glycerol-based processes, respectively. The distillate rate was calculated *via* a preliminary balance using the shortcut model, whose results are shown in the supplementary information section B. Sensitivity analysis determining the effect of the distillate rate, the number of stages and reflux ratios on the efficiency of the separation are included in the supplementary information section B. The sizing was performed to ensure maximum recoveries of the components such as acrolein, AA and the solvents were attained.

The results in Tables 7 and 8 illustrate that overall, the columns in the glycerol-based process are less complex as the columns have a lower number of stages, operate at lower pressures (excluding vacuum operating columns), and have lower distillate rates. As a result, advantages such as less material for construction is required, and lower condenser and reboiler duties can be attained.

4.3. Comparison of the two processes

The detailed mass balance tables of all the streams are available in the supplementary information sections C and D. Based on Table 9 and Table 10, the propylene and glycerol-based routes generate 10233.4 kg h^{-1} and 10226.0 kg h^{-1} of AA, respectively, in both cases at a purity greater than 99.5 wt%, thus complying with industrial standard specifications.

To achieve the required AA purity in the propylene-based route, the LL extractor (P_E1), solvent recovery column (P_D1), and raffinate column (P_D2) column, has an overall AA recovery of 99.9 wt%. Whilst, in the glycerol-based route, the azeotropic distillation (G_D2) column has 100.0% of AA recovery. Furthermore, from the mass balance results, Fig. 4 illustrates the raw materials consumed and waste disposed of per kg of AA.

Fig. 4 shows that the propylene-based process utilises less feedstock to achieve an equivalent production of AA, this being 0.92 kg h^{-1} of propylene as opposed to 2.31 kg h^{-1} of glycerol. The difference in the amount of raw material is expected to be due to the nature of the glycerol molecule compared to propylene as presented in reactions (1) and (4) mainly because of the oxygen content in glycerol. Moreover, Fig. 4 considers the total amount of steam that is used in the reaction units and water used for quenching, as well as the total amount of air streams that are used for the reaction unit and in the fired heaters. The results illustrate that for 1 kg h^{-1} of AA, 2.47 kg h^{-1} and 2.01 kg h^{-1} of steam/water are utilised in the propylene and glycerol-based processes, respectively. This is due to the quenching unit consuming 9000 kg h^{-1} of water in the propylene route compared to 500 kg h^{-1} of water consumed in the glycerol route. However, when comparing the amount of wastewater generated (due to the dehydration (4)), the glycerol route generates more wastewater (3.37 kg h^{-1}) compared to the 2.84 kg h^{-1} generated by the propylene route.

Whilst, 11.43 kg h^{-1} and 5.55 kg h^{-1} of air are consumed in the propylene and glycerol routes, respectively. This is expected, as the propylene route employs two oxidation reactors and three fired heaters are needed to flare waste products, compared to the glycerol route where one oxidation reactor and one fired heater are required. This also leads the propylene route to generate 11.04 kg h^{-1} of waste/flue gases, which consists of 1.11 kg h^{-1} of CO_2, compared to the glycerol route which generates 5.53 kg h^{-1} of waste/flue gases, consisting of 0.68 kg h^{-1} of CO_2. In addition, indirect CO_2 emissions associated with utilities were calculated during the heat integration analysis and discussed in Section 4.4. CO_2 emissions from the glycerol route attained in this study were compared to results presented by Dimian and Bildea (2021). In this

Table 9
Mass Balance results for the overall inputs and outputs of the propylene-based process.

Stream	1	2	3	12	15	16	26	27	29	34	35	36	38	39
Temperature (°C)	25.0	160.0	25.0	25.0	25.0	100.0	25.0	100.0	95.6	25.0	100.0	25.0	45.9	100.4
Pressure (bar)	11.5	6.0	1.0	6.8	1.0	1.0	1.0	1.0	1.1	1.0	1.0	1.0	0.1	0.2
Molar Vapor Fraction	1.0	1.0	1.0	0.0	1.0	1.0	1.0	1.0	0.0	1.0	1.0	0.0	0.0	0.0
Enthalpy (MJ $kmol^{-1}$)	13.4	−237.2	0.0	−285.8	0.0	−35.4	0.0	−58.5	−279.9	0.0	−60.9	−350.8	−286.1	−359.1
Mole Flow (kmol h^{-1})	225.8	903.2	2416.1	499.6	1229.1	3490.0	304.8	332.0	1301.8	103.7	112.2	4.9	293.4	141.9
Components mole fraction														
Water	–	1.0	–	1.0	–	0.05	–	0.10	0.99	–	0.10	–	0.99	–
Acetic Acid	–	–	–	–	–	–	–	–	trace	–	–	–	0.01	
AA	–	–	–	–	–	–	–	–	–	–	–	–	–	1.00
Carbon Dioxide	–	–	–	–	–	0.06	–	0.09	–	–	0.10	–	–	–
Acrolein	–	–	–	–	–	–	–	–	–	–	–	–	–	–
DIPE	–	–	–	–	–	–	–	–	–	–	–	1.0	–	–
Propylene	0.94	–	–	–	–	–	–	–	–	–	–	–	–	–
Oxygen	–	–	0.21	–	0.21	0.06	0.21	0.06	–	0.21	0.06	–	–	–
Nitrogen	–	–	0.79	–	0.79	0.82	0.79	0.74	–	0.79	0.74	–	–	–
Propane	0.03	–	–	–	–	–	–	–	–	–	–	–	–	–
Ethane	0.03	–	–	–	–	–	–	–	–	–	–	–	–	–
Acetaldehyde	–	–	–	–	–	–	–	–	–	–	–	–	–	–
Carbon monoxide	–	–	–	–	–	–	–	–	–	–	–	–	–	–
Formaldehyde	–	–	–	–	–	–	–	–	–	–	–	–	–	–

Table 10
Mass Balance results for the overall inputs and outputs of the Glycerol-based process.

Stream	1	3	5	10	11	18	26	28	29	32	33
Temperature (°C)	25.0	159.0	25.0	101.2	25.0	25.0	100.0	15.0	25.0	54.0	103.2
Pressure (bar)	1.0	6.0	1.0	1.0	1.0	1.0	1.0	0.3	0.3	0.2	0.3
Molar Vapor Fraction	0.0	1.0	1.0	0.0	1.0	0.0	1.0	0.0	0.0	0.0	0.0
Enthalpy (MJ kmol^{-1})	−485.6	−238.0	−0.6	−283.0	−0.6	−285.9	−39.1	−268.1	12.2	−283.8	−378.2
Mole Flow (kmol h^{-1})	414.1	1112.9	90.7	1709.1	1875.1	27.8	1930.0	70.1	4.3	31.3	141.9
Components mole fraction											
Glycerol	0.53	–	–	–	–	–	–	–	–	–	–
Acrolein	–	–	–	–	–	–	–	–	–	–	–
Water	0.47	1.0	–	0.98	–	1.0	0.04	0.89	–	1.0	–
Acetaldehyde	–	–	–	–	–	–	–	–	–	–	–
Carbon Monoxide	–	–	–	–	–	–	–	–	–	–	–
Propionic acid	–	–	–	0.01	–	–	–	–	–	–	–
Oxygen	–	–	0.21	–	0.21	–	0.08	–	–	–	–
Carbon Dioxide	–	–	–	–	–	–	0.08	–	–	–	–
Nitrogen	–	–	0.79	–	0.79	–	0.80	0.07	–	–	–
Hydrogen	–	–	–	–	–	–	–	–	–	–	–
AA	–	–	–	–	–	–	–	–	–	trace	1.00
Acetic Acid	–	–	–	–	–	–	–	–	–	–	–
Toluene	–	–	–	–	–	–	–	–	1.0	–	–
Acetol	–	–	–	0.01	–	–	–	–	–	–	–
Acetone	–	–	–	–	–	–	–	0.04	–	–	–

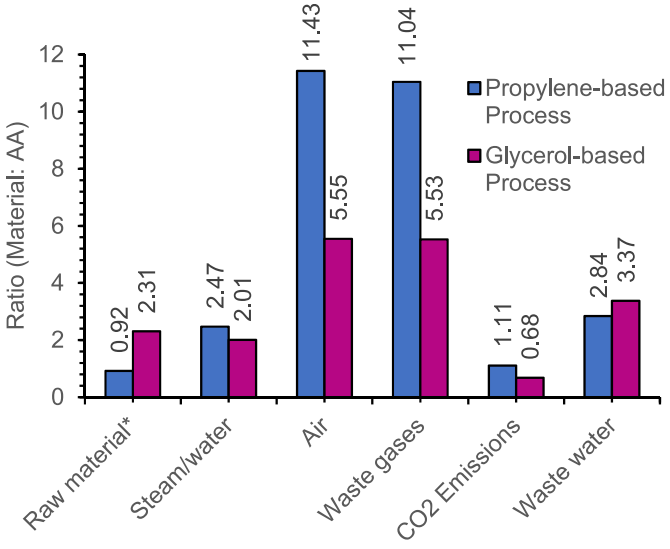

Fig. 4. Mass Balance results per 1 kg of AA. *Raw material indicates chemical grade propylene (94 wt% purity) and glycerol aqueous solution (85 wt % glycerol).

work, 0.68 kg of CO_2 per kg of AA are emitted compared to 0.23 kg CO_2 per kg of AA, because in this study the offgas combustion and incineration are also considered along with the CO_2 generated by the process. Excluding CO_2 emissions due to combustion, results are very close 0.27 kg CO_2 per kg of AA.

To account for the uncertainties associated with the kinetic model, a sensitivity analysis was performed by keeping operating conditions constant and varying the kinetic values (i.e. pre-exponential factors) to observe the impact on selectivity towards acrolein (reactions (1)(2)(4)). This analysis also represented the impact of possible catalyst deactivation (Martín et al., 2022) during the material lifetime.

Fig. 5 illustrates the amount of AA generated from the reaction unit before purification and the amount of CO_2 emissions generated from the overall process when varying the selectivity of reactions (1) and (4). The results show that as the selectivity increases to about 80%, the amount of AA produced in the propylene and glycerol routes also increases, with the glycerol route generating more AA compared to propylene. This is because at selectivity lower than 80%, the overall conversion of glycerol achieved in the dehydration reactor (G_R1) is higher than the overall conversion of propylene attained in the oxidation reactor (P_R1). For example, it was found that at selectivity of 60%, the conversion of glycerol was 91%, while the conversion of propylene was 35.6%. However, at selectivity above 80% (which is comparable with industrial experience (Redlingshöfer et al., 2002)), the propylene route generates more AA (Fig. 5a). This is because the reactor P_R1 also generates AA in a side reaction which becomes more prominent at higher selectivity, while the reactor G_R1 does not. For example, when the selectivity is about 80%, it can be observed that the conversion of propylene is slightly lower (92.2%) compared to glycerol (98.6%).

Moreover, analysing Fig. 5b, shows that, regardless of selectivity, the propylene route generates more CO_2 due to reasons discussed earlier.

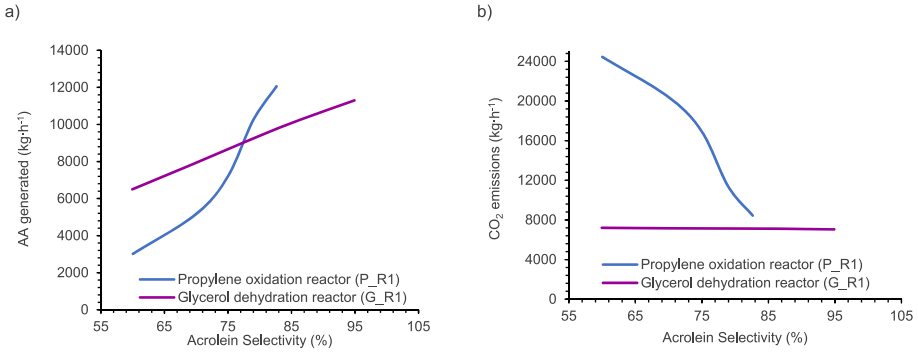

Fig. 5. a) Sensitivity of AA production at different acrolein selectivity; b) Sensitivity of direct CO_2 emissions at different acrolein selectivity.

When increasing selectivity, it is observed that CO_2 emissions decrease in the propylene-based process. Recycling propylene back to the reactor could partially reduce emissions at low selectivity providing that the low-temperature separation of propylene from other uncondensable gases (O_2, N_2, etc.) is not cost-prohibitive. When evaluating the glycerol-based process, it is observed that CO_2 emissions are not affected by selectivity. This can be explained since at lower selectivity, side reactions in G_R1 generate more CO and acetone which are later separated and flared in the form of CO_2. However, at higher selectivity, more acrolein is generated and converted in the oxidation reactor (G_R2) where both the yield of AA and CO_2 increases.

Varying the selectivity towards AA (reaction (2) in the oxidation reactors (P_R2 and G_R2), the following results illustrated in Fig. 6 are attained. From Fig. 6a, it is observed that when increasing the selectivity towards AA, the production of AA also increases in both processes. This is expected as the increase of the selectivity of the reaction ((2) turns into a higher conversion of acrolein into AA. It can also be observed that both processes generate nearly an equal amount of AA regardless of the selectivity. This is because both oxidation reactors (P_R2 and G_R2) behave similarly when the kinetics and selectivity of the reaction vary. Furthermore, it can be observed from Fig. 6b, that in both routes as selectivity increases, CO_2 emissions decrease. This is because, at higher selectivity, acrolein primarily takes part in the main reaction to generate AA instead of taking part in the side reactions that produce CO_x.

4.4. Heat integration results

Fig. 7 shows the grant composite curves (GCC) of the propylene and glycerol-based routes, respectively. The hot utility is required to be at a temperature higher than 488 °C and 505 °C for the propylene and glycerol routes, respectively. While the cold utility is required to be at a temperature lower than −0.5 °C and 9.5 °C for the propylene and glycerol-based processes respectively.

Table 11 summarizes the heat integration results. Since natural gas combustion is considered a high-temperature heat source, additional indirect CO_2 emissions are considered from the processes. For the propylene route, the heating demand can be accomplished *via* heat integration (thus minimum hot utility = 0 MW). Instead, an additional 16.4 kg of CO_2 per ton of AA are emitted for the glycerol route exclusively from the external fired heaters that are operated with natural gas while the CO_2 from the process emitted from the incineration of waste steams is originated from biogenic sources and therefore is carbon neutral.

Finally, Fig. 8 compares the energy saving opportunities of both routes using the results in Table 11. Table 12 summarizes the number of heat transfer equipment required by each route.

In the propylene route, heating energy can be completely extracted from the 11 hot streams (shown in Table 12) to fulfil the heating demand required by the 4 cold streams (3 reboilers and 1 heater). Whilst in the glycerol route, heating demand is slightly higher (27.8 MW) as opposed to the propylene route (25.3 MW) due to the presence of 3 reboilers of the distillation columns and 3 heaters used to heat raw materials.

However, when comparing cooling energy savings, the glycerol-based process shows higher savings of (32.4%) as opposed to the propylene route (21.6%). In the propylene route, the hot streams release more heat at higher temperatures, for example, the process has two oxidation reactors that are exothermic at temperatures of 366 °C and 375 °C. The heat from the reactors can be utilised to generate MP steam at 250 °C. The process also includes three fired heaters that generate flue gases thus require more cooling utility to extract that heat. Whilst the glycerol route, has one exothermic reactor and one fired heater, requiring less cooling demand and utility.

Furthermore, the heating energy savings for the glycerol route were compared to the results by Dimian and Bildea (2021). The reference indicated that extracting the heat from the reactors leads to 80% heating energy savings which is slightly lower than the optimisation carried out in this work because other heat sources in the separation unit were

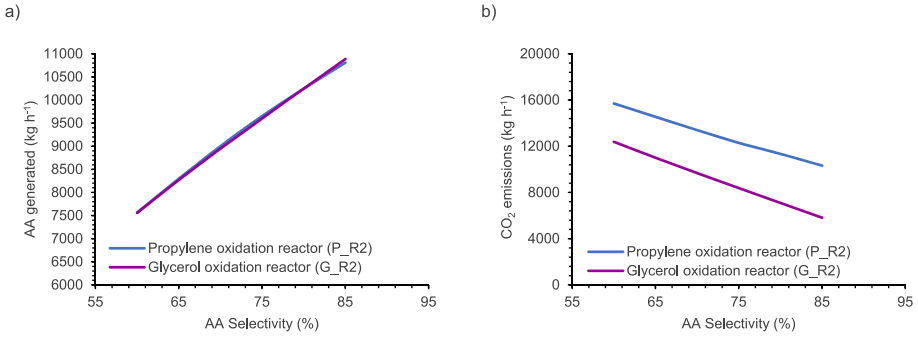

Fig. 6. a) AA generated at increased AA selectivity; b) CO_2 emissions at different AA selectivity.

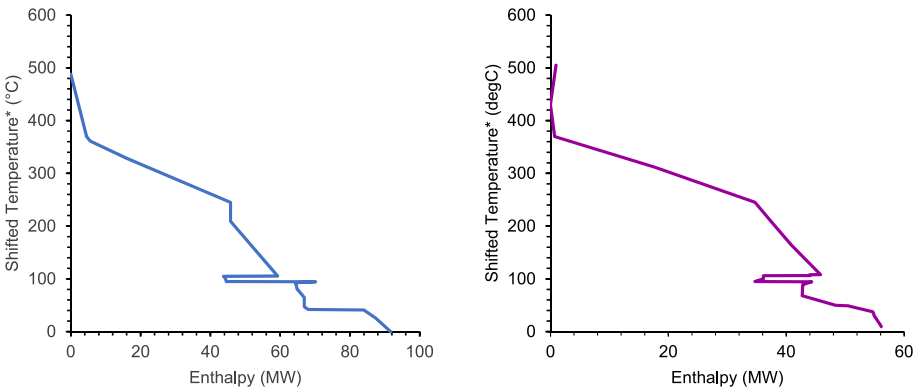

Fig. 7. Grant composite curves for the propylene route (left) and for the glycerol route (right).

Table 11
Heat integration results.

	Propylene Route	Glycerol Route
Pinch temperature (°C)	487.9	430.2
Minimum hot utility (MW)	0.0	0.95
Minimum cold utility (MW)	91.7	56.1
Heat demand from Aspen Plus (MW)	25.3	27.8
Cooling demand from Aspen Plus (MW)	117.0	83.0

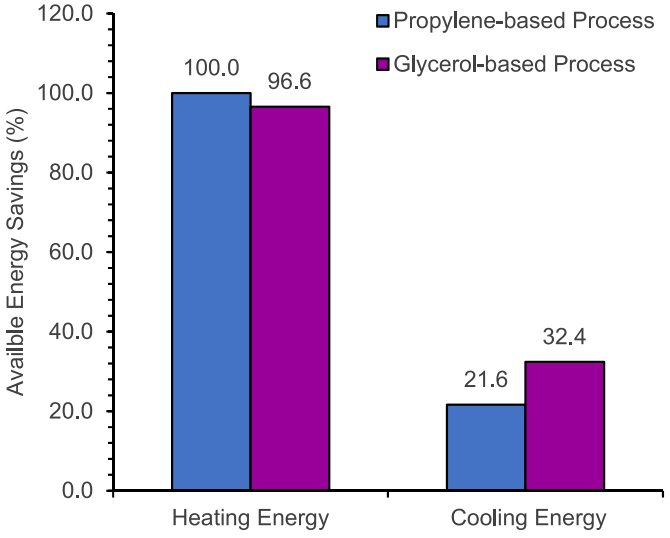

Fig. 8. Comparison of the energy saving opportunities.

Table 12
Number of heating and cooling equipment implemented by both processes.

Equipment	Propylene Route	Glycerol Route
Heaters	1	3
Coolers	4	4
Condensers	2	2
Reboilers	3	3
Fired heaters	3	1
Exothermic reactor	2	1

considered along with the heat extracted from the reactor.

4.5. Economic analysis results

The economic comparison of the two processes is reported in Fig. 9.

The results illustrate that the propylene-based process requires higher CAPEX (£91.3 million) compared to the glycerol-based process (£74.0 million). This is due to the more capital-intensive AA recovery *via* LL extraction in the propylene route which comprises two distillation columns to recover and recycle the solvent back to the extractor compared to the azeotropic distillation employed in the glycerol one.

Moreover, the propylene-based route requires higher OPEX (£180.2 million yr^{-1}) compared to the glycerol-based route (£171.4 million yr^{-1}). This is mainly due to the difference in utility cost, in which more cooling utilities in the form of refrigeration are required in the propylene-based process as discussed earlier in section 4.4. However, when considering raw materials independently, the propylene route has a lower cost (£117.2 million yr^{-1}) compared to the glycerol route (£138.6 million yr^{-1}). This is expected, as more glycerol (20,050 kg h^{-1}) is utilised in the process compared to propylene (9434 kg h^{-1}). Whilst maintenance costs are slightly higher for the propylene-based route (£3.70 million yr^{-1}) compared to the glycerol-based process (£3.0 million yr^{-1}) due to the difference in the total investment cost.

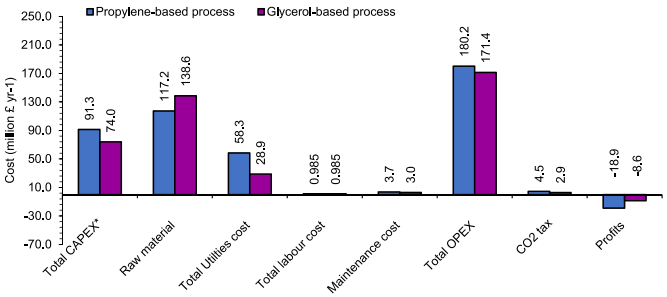

Fig. 9. Economic analysis results. NOTE: *CAPEX is expressed in millions of £

Moreover, assuming a CO_2 emission tax of £50 ton^{-1} of CO_2 , it is found that the propylene route has a higher total annualised cost due to CO_2 tax (£4.5 million yr^{-1}) compared to the glycerol route (£2.9 million yr^{-1}). This is expected as a total of 90873.0 tons yr^{-1} of CO_2 are generated from the propylene route as opposed to the glycerol route which generates 57332.9 tons yr^{-1} of CO_2, which includes CO_2 generated from utilities as discussed earlier.

Based on the costs and assumptions made in this study, both processes do not generate profits because of the high cost of the raw materials. However, due to the difference in OPEX, especially due to utility cost, as well as the total cost of CO_2 emissions the propylene route is below the breakeven point by £-18.9 million yr^{-1} compared to the glycerol route (£-8.6 million yr^{-1}). Moreover, the results attained in this study for the glycerol route were compared to the analysis presented by the base case study (Dimian et al., 2019). The capital cost attained (£74.0 million) is slightly higher than the cost attained in the base case study (£69.3 million), mainly due to the difference in equipment sizing. Utility cost attained (£28.9 million yr^{-1}) is much higher compared to the base case study (£4.25 million yr^{-1}) due to cooling utility demand. Finally, raw material cost calculated is also higher (£138.6 million yr^{-1}) as opposed to the base case (£26.5 million yr^{-1}). This is due to the difference in the assumption for the cost of glycerol (≈×2.3 times).

To further investigate the effect of a CO_2 tax on the total cost of CO_2 emissions, a sensitivity analysis was performed and it is shown in Fig. 10 considering a wide range of carbon tax (Department for Business, 2020). As shown in Fig. 10, varying the tax cost from 0 to 300 £ $ton^{-1}_{(CO2)}$, the total cost of CO_2 emissions for the propylene and glycerol routes increase to £27.3 million yr^{-1} and £17.2 million yr^{-1}, respectively. This is due to the difference in the amount of CO_2 generated in both processes.

Fig. 11(left) illustrates the results of the sensitivity analysis

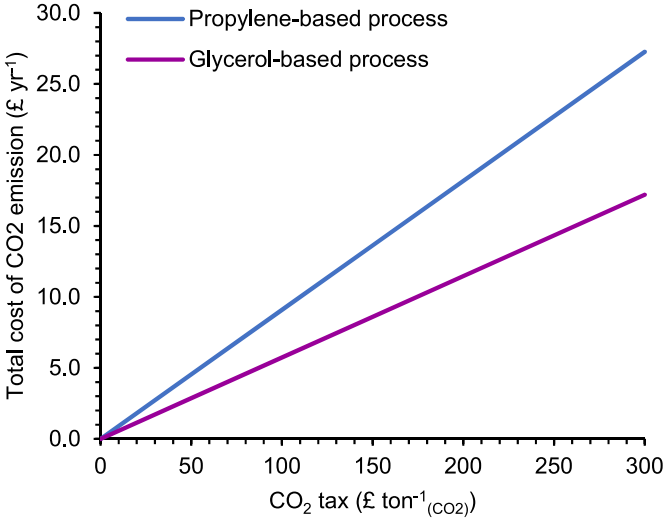

Fig. 10. Effect of CO_2 tax on total cost spent due to CO_2 emissions.

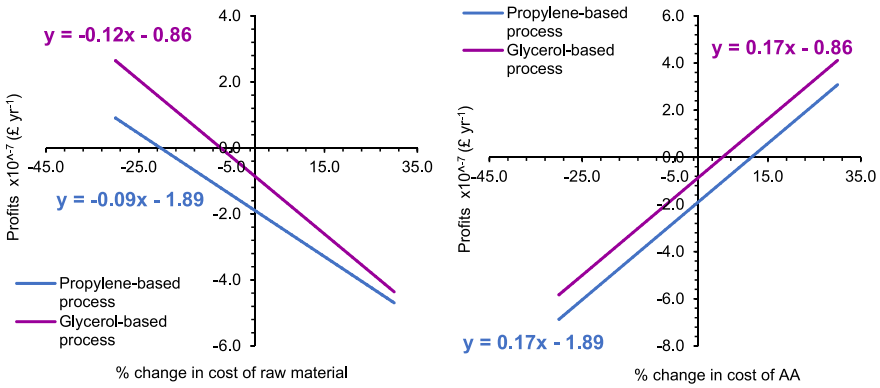

Fig. 11. left) Raw material effect on process profits, right) Effect of AA cost on process profits.

performed to determine the effects of cost variations of raw materials (propylene and glycerol) on the profits gained. The slopes of the line illustrate that an increase in propylene cost has a lesser effect on profits compared to glycerol. This is because the cost of propylene is 47% of the total OPEX, while the cost of glycerol is 62% of the total OPEX. Moreover, Fig. 11(right) illustrates the results of the sensitivity analysis performed to determine the effects of cost variations of AA on the profit whilst keeping OPEX and CO_2 emission cost constant at the base case. From Fig. 11 (right) it can be noted that the AA breakeven price is achieved at 11% higher than the base case, while for glycerol, this is limited to a maximum increase of 5% of the value set as in the base case.

5. Conclusions

This work has demonstrated that bio-based feedstock is a viable option to replace propylene for the production of AA. This is due to glycerol being available in large volumes as biogenic waste, thus more environmentally friendly and more resilient to socio-economic and geo-political events. As glycerol production from biodiesel is not centralised and often randomly distributed across a country, this could result in a substantial barrier for the feedstock supply chain.

Process integration and optimisation have shown that the glycerol-based process can attain heating and cooling energy savings of 96.6% and 32.4%, respectively. While the propylene-based process attains heating and cooling energy savings of 100% and 21.6%, respectively. In addition, the use of glycerol as feedstock would reduce direct and indirect CO_2 emissions by 414 kg per ton of AA.

The techno-economic analysis results show that the CAPEX of the propylene-based process is 23.4% higher than the glycerol-based route. As glycerol-to-AA is still not commercially available those results may deviate substantially from the actual costs of construction. In case of the propylene route, variations in reactor performance and associated costs and carbon tax have the highest impact.

The main barriers to enabling this process towards commercialisation are represented by: i) material and catalyst stability to obtain long terms operation at high AA yield, ii) an established supply chain for the glycerol feedstock, including cost fluctuation and feedstock specification which can change significantly depending on the biodiesel plant; iii) the implementation of environmental policy to consider the cost of CO_2 emissions as well as new incentives to push industries towards bio-based applications; iv) market and infrastructure constraints, especially in Europe or UK, where import from Asia or America is often the preferred route to afford the cost of new installations.

Future works are currently looking at the proof-of-concept of a new intensified glycerol-to-acrylic acid process that could reduce the number of conversion and separation processes, and the cost of utilities. In this respect, the results in terms of process integration will include the impact of different glycerol purity and the expected cost for the required purification as well as the opportunity for heat integration and heat exchange network design.

CRediT authorship contribution statement

Aya Sandid: Conceptualization, Methodology, Software, Data curation, Writing – original draft. **Jesús Esteban:** Revision, Investigation, Funding acquisition, Supervision. **Carmine D'Agostino:** Revision, Investigation, Funding acquisition. **Vincenzo Spallina:** Supervision, Conceptualization, Funding acquisition, Writing – review & editing.

Declaration of competing interest

The authors declare that they have no known competing financial interests or personal relationships that could have appeared to influence the work reported in this paper.

Data availability

Data will be made available on request.

Acknowledgements

The authors would like to acknowledge the financial support from the UKRI-EPSRC SPACING project, EP/V026089/1. The School of Engineering at the University of Manchester is acknowledged for sponsoring the PhD scholarship of Aya Sandid. In addition, support from the SPRINT program jointly funded by The University of Manchester and FAPESP is gratefully acknowledged.

Appendix A. Supplementary data

Supplementary data to this article can be found online at https://doi.org/10.1016/j.jclepro.2023.138127.

References

Vallero, D.A., 2019. Air Pollution Calculations - Thermal Reactions. Elsevier Inc.
Alvarez, M.E., Moraes, E.B., Machado, A.B., Maciel Filho, R., Wolf-Maciel, M.R., 2007. Evaluation of liquid-liquid extraction process for separating acrylic acid produced from renewable sugars. Appl. Biochem. Biotechnol. 137–140 (1–12), 451–461. https://doi.org/10.1007/s12010-007-9071-1.
Arntz, D., Fischer, A., Höpp, M., Jacobi, S., Sauer, J., Ohara, T., Sato, T., Shimizu, N., Schwind, H., 2007. Acrolein and Methacrolein, Ullmann's Encyclopedia of Industrial Chemistry.
Attarbachi, T., Kingsley, M.D., Spallina, V., 2023. New trends on crude glycerol purification: a review. Fuel 340, 127485. https://doi.org/10.1016/j.fuel.2023.127485.
Bhagyashri Patil, P.M., Prasad, Eswara, 2022. Acrylic Acid Market.
Braga, E., Mustafa, G., Pontes, D., Pontes, L.A.M., 2020. Economic analysis and technicalities of acrylic acid production from crude glycerol. Chem. Ind. Chem. Eng. Q. 26, 59–69. https://doi.org/10.2298/CICEQ180111025B.

Brennan, D., 2020. Chapter 4 - operating cost estimation. In: Brennan, D. (Ed.), Process Industry Economics, second ed. Elsevier, pp. 95–125.
Brown, D., 2014. Acrylic acid. In: Wexler, P. (Ed.), Encyclopedia of Toxicology, third ed. Academic Press, Oxford, pp. 74–75.
ChemAnalyst, 2022a. Acrylic acid price trend and forecast. https://www.chemanalyst.com/Pricing-data/acrylic-acid-20. (Accessed 26 July 2022).
ChemAnalyst, 2022b. Diisopropyl ether price trend and forecast. https://www.chemanalyst.com/Pricing-data/diisopropyl-ether-1137%20. (Accessed 26 July 2022).
ChemAnalyst, 2022c. Propylene price trend and forecast. https://www.chemanalyst.com/Pricing-data/propylene-51. (Accessed 26 July 2022).
Chemical Engineering, 2022. Economic Indicators, p. 52.
Chilakamarry, C.R., Sakinah, A.M.M., Zularisam, A.W., Pandey, A., 2021. Glycerol waste to value added products and its potential applications. Syst. Microbiol. Biomanufact. 1 (4), 378–396. https://doi.org/10.1007/s43393-021-00036-w.
Choi, Y.B., Nunotani, N., Morita, K., Imanaka, N., 2022. Selective glycerol oxidation to glyceric acid under mild conditions using Pt/CeO2-ZrO2-Fe2O3/SBA-16 catalysts. J. Asian Ceram. Soc. 10 (1), 178–187. https://doi.org/10.1080/21870764.2022.2028980.
Cornejo, A., Barrio, I., Campoy, M., Lázaro, J., Navarrete, B., 2017. Oxygenated fuel additives from glycerol valorization. Main production pathways and effects on fuel properties and engine performance: a critical review. Renew. Sustain. Energy Rev. 79, 1400–1413. https://doi.org/10.1016/j.rser.2017.04.005.
Department for Business, E.I.S., 2020. Updated Energy and Emission Projections: 2019. Annex M.
Department for Business, E.I.S., 2022. Prices of Fuels Purchased by the Manufacturing Industry in Great (Britain).
Dimian, A.C., Bildea, C.S., 2021. Sustainable process design for manufacturing acrylic acid from glycerol. Chem. Eng. Res. Des. 166, 121–134. https://doi.org/10.1016/j.cherd.2020.12.002.
Dimian, A.C., Bildea, C.S., Kiss, A.A., 2019. 14 - acrylic acid. In: Dimian, A.C., Bildea, C. S., Kiss, A.A. (Eds.), Applications in Design and Simulation of Sustainable Chemical Processes. Elsevier, pp. 521–569.
Drochner, A., Kampe, P., Menning, N., Blickhan, N., Jekewitz, T., Vogel, H., 2014. Acrolein oxidation to acrylic acid on Mo/V/W-mixed oxide catalysts. Chem. Eng. Technol. 37 (3), 398–408. https://doi.org/10.1002/ceat.201300797.
Echemi Technology, 2022. Toluene international price. https://www.echemi.com/pip/toluene-temppid160704000607.html. (Accessed 1 August 2022).
Esteban, J., Fuente, E., Blanco, A., Ladero, M., Garcia-Ochoa, F., 2015a. Phenomenological kinetic model of the synthesis of glycerol carbonate assisted by focused beam reflectance measurements. Chem. Eng. J. 260, 434–443. https://doi.org/10.1016/j.cej.2014.09.039.
Esteban, J., Ladero, M., Garcia-Ochoa, F., 2015b. Kinetic modeling of the solventless synthesis of solketal with a sulphonic ion exchange resin. Chem. Eng. J. 269, 194–202. https://doi.org/10.1016/j.cej.2015.01.107.
European Basic Acrylic Monomer Group (EBAM), 2012. Safe handling and storage of acrylic acid. In: Acrylic Acid and Esters Chemical Economics Handbook, third ed. IHS Markit. 2020.
Indeed, 2022a. Maintenance engineer salary in United Kingdom. https://uk.indeed.com/career/maintenance-engineer/salaries. (Accessed 26 July 2022).
Indeed, 2022b. Maintenance technician salary in United Kingdom. https://uk.indeed.com/career/maintenance-technician/salaries. (Accessed 26 July 2022).
Indeed, 2022c. Plant manager salary in United Kingdom. https://uk.indeed.com/career/plant-manager/salaries. (Accessed 26 July 2022).
Indeed, 2022d. Plant operator salary in United Kingdom. https://uk.indeed.com/career/plant-operator/salaries. (Accessed 26 July 2022).
Kumar, L.R., Tyagi, R.D., Drogui, P., 2021. Economic Analysis for Simultaneous Production of Microbial Lipid and Citric Acid by Oleaginous Yeast Cultivated on Purified Crude Glycerol. Biomass Conversion and Biorefinery. https://doi.org/10.1007/s13399-021-01772-8.
Liu, L., Ye, X.P., Bozell, J.J., 2012. A comparative review of petroleum-based and bio-based acrolein production. ChemSusChem 5 (7), 1162–1180. https://doi.org/10.1002/cssc.201100447.
Luyben, W.L., 2016. Economic trade-offs in acrylic acid reactor design. Comput. Chem. Eng. 93, 118–127. https://doi.org/10.1016/j.compchemeng.2016.06.005.
Martín, A.J., Mitchell, S., Mondelli, C., Jaydev, S., Pérez-Ramírez, J., 2022. Unifying views on catalyst deactivation. Nat. Catal. 5 (10), 854–866. https://doi.org/10.1038/s41929-022-00842-y.
Ohara, T., Sato, T., Shimizu, N., Prescher, G., Schwind, H., Weiberg, O., Marten, K., Greim, H., Shaffer, T.D., Nandi, P., 2020. Acrylic Acid and Derivatives, Ullmann's Encyclopedia of Industrial Chemistry, pp. 1–21.
Petrescu, L., Fermeglia, M., Cormos, C.C., 2016. Life Cycle Analysis applied to acrylic acid production process with different fuels for steam generation. J. Clean. Prod. 133, 294–303. https://doi.org/10.1016/j.jclepro.2016.05.088.
Pico, M.P., Rodríguez, S., Santos, A., Romero, A., 2013. Etherification of glycerol with benzyl alcohol. Ind. Eng. Chem. Res. 52 (41), 14545–14555. https://doi.org/10.1021/ie402026t.
Premlall, K.C., Lokhat, D., 2020. Reducing energy requirements in the production of acrylic acid: simulation and design of a multitubular reactor train. Energies 13 (8), 1971. https://doi.org/10.3390/en13081971.
R Kumar, L., Yellapu, S., Tyagi, R.D., Drogui, P., 2020. Purified crude glycerol by acid treatment allows to improve lipid productivity by Yarrowia lipolytica SKY7. Process Biochem. 96, 165–173. https://doi.org/10.1016/j.procbio.2020.06.010.
Redlingshöfer, H., Fischer, A., Weckbecker, C., Huthmacher, K., Emig, G., 2003. Kinetic modeling of the heterogeneously catalyzed oxidation of propene to acrolein in a catalytic wall reactor. Ind. Eng. Chem. Res. 42 (22), 5482–5488. https://doi.org/10.1021/ie030191p.
Redlingshöfer, H., Kröcher, O., Böck, W., Huthmacher, K., Emig, G., 2002. Catalytic wall reactor as a tool for isothermal investigations in the heterogeneously catalyzed oxidation of propene to acrolein. Ind. Eng. Chem. Res. 41 (6), 1445–1453. https://doi.org/10.1021/ie0106074.
Ruy, A.D.d.S., Ferreira, A.L.F., Bresciani, A.É., de Brito Alves, R.M., Pontes, L.A.M., 2020. Market prospecting and assessment of the economic potential of glycerol from biodiesel. Intech.
Sánchez-Gómez, J.A., Cabrera-Ruiz, J., Hernández, S., 2022. Design and optimization of an intensified process to produce acrylic acid as added product value from glycerol generated in the biodiesel production. Chem. Eng. Res. Des. 184, 543–553. https://doi.org/10.1016/j.cherd.2022.06.032.
Sinnott, R.K., Towler, G.P., 2020. Chemical Engineering Design, sixth ed. Butterworth-Heinemann, an imprint of Elsevier, Kidlington, Oxford, United Kingdom.
Smith, R., 2005. Chemical Process Design and Integration. John Wiley & Sons, Incorporated, New York.
Song, D., Yang, J.-H., Lee, C.-J., 2020. Conceptual design of water separation process in glycerol-based acrylic acid production. Chem. Eng. Res. Des. 156, 324–332. https://doi.org/10.1016/j.cherd.2020.01.036.
Stenberg, V., Spallina, V., Mattisson, T., Rydén, M., 2021. Techno-economic analysis of processes with integration of fluidized bed heat exchangers for H2 production – Part 2: chemical-looping combustion. Int. J. Hydrogen Energy 46 (50), 25355–25375. https://doi.org/10.1016/j.ijhydene.2021.04.170.
Suo, X., Zhang, H., Ye, Q., Dai, X., Yu, H., Li, R., 2015. Design and control of an improved acrylic acid process. Chem. Eng. Res. Des. 104, 346–356. https://doi.org/10.1016/j.cherd.2015.08.022.
Talebian-Kiakalaieh, A.A.N., 2017. Kinetic study on catalytic conversion of glycerol to renewable acrolein. Chem. Eng. Trans. 56, 655–660. https://doi.org/10.3303/CET1756110.
U.S. Energy Information Administration (EIA), 2019. EIA projects nearly 50% increase in world energy usage by 2050, led by growth in Asia. https://www.eia.gov/todayinenergy/detail.php?id=42342#:~:text=EIA%20projects%20nearly%2050%25%20increase,led%20by%20growth%20in%20Asia&text=From%20December%2023%20through%20January,originally%20published%20on%20Septmber%2024. (Accessed 11 July 2022).
U.S. Energy Information Administration (EIA), 2021. International Energy Outlook 2021 with Projections to 2050.
University of Manchester, 2022. Sprint.
Wu, S.T., She, Q.M., Tesser, R., Serio, M.D., Zhou, C.H., 2020. Catalytic glycerol dehydration-oxidation to acrylic acid. Catal. Rev. 62 (4), 481–523. https://doi.org/10.1080/01614940.2020.1719611.
Xiao, Y., Xiao, G., Varma, A., 2013. A universal procedure for crude glycerol purification from different feedstocks in biodiesel production: experimental and simulation study. Ind. Eng. Chem. Res. 52 (39), 14291–14296. https://doi.org/10.1021/ie402003u.